Original Article | Cardiovascular Imaging

eISSN 2005-8330
https://doi.org/10.3348/kjr.2018.0251
Korean J Radiol 2019;20(1):94-101

Korean Journal of Radiology
KJR

Influence of Heart Rate and Innovative Motion-Correction Algorithm on Coronary Artery Image Quality and Measurement Accuracy Using 256-Detector Row Computed Tomography Scanner: Phantom Study

Jeong Bin Park, MD, Yeon Joo Jeong, MD, PhD, Geewon Lee, MD, PhD, Nam Kyung Lee, MD, PhD, Jin You Kim, MD, PhD, Ji Won Lee, MD, PhD

All authors: Department of Radiology, Pusan National University School of Medicine and Medical Research Institute, Pusan National University Hospital, Busan, Korea

Objective: To investigate the efficacy of motion-correction algorithm (MCA) in improving coronary artery image quality and measurement accuracy using an anthropomorphic dynamic heart phantom and 256-detector row computed tomography (CT) scanner.

Materials and Methods: An anthropomorphic dynamic heart phantom was scanned under a static condition and under heart rate (HR) simulation of 50–120 beats per minute (bpm), and the obtained images were reconstructed using conventional algorithm (CA) and MCA. We compared the subjective image quality of coronary arteries using a four-point scale (1, excellent; 2, good; 3, fair; 4, poor) and measurement accuracy using measurement errors of the minimal luminal diameter (MLD) and minimal luminal area (MLA).

Results: Compared with CA, MCA significantly improved the subjective image quality at HRs of 110 bpm (1.3 ± 0.3 vs. 1.9 ± 0.8, $p = 0.003$) and 120 bpm (1.7 ± 0.7 vs. 2.3 ± 0.6, $p = 0.006$). The measurement error of MLD significantly decreased on using MCA at 110 bpm (11.7 ± 5.9% vs. 18.4 ± 9.4%, $p = 0.013$) and 120 bpm (10.0 ± 7.3% vs. 25.0 ± 16.5%, $p = 0.013$). The measurement error of the MLA was also reduced using MCA at 110 bpm (19.2 ± 28.1% vs. 26.4 ± 21.6%, $p = 0.028$) and 120 bpm (17.9 ± 17.7% vs. 34.8 ± 19.6%, $p = 0.018$).

Conclusion: Motion-correction algorithm can improve the coronary artery image quality and measurement accuracy at a high HR using an anthropomorphic dynamic heart phantom and 256-detector row CT scanner.

Keywords: *Tomography; X-ray computed; Coronary vessels; Phantoms; Imaging; Motion-correction algorithm; Heart rate*

INTRODUCTION

Computed tomography (CT) has been widely utilized as a non-invasive diagnostic modality for visualizing coronary arteries and excluding coronary artery diseases. However, motion artifacts caused by rapid cardiac movements remain a major challenge for better image quality and higher diagnostic accuracy in predicting coronary artery disease (1, 2).

To reduced motion artifact and improve diagnostic accuracy, CT scanners with higher temporal resolutions and wide detector arrays have been developed. In addition to this hardware development, motion-correction algorithm (MCA) has recently been introduced to compensate for coronary motion artifacts. MCA can characterize vessel motions (both path and velocity) using information from adjacent cardiac phases within a single cardiac cycle and determine the actual vessel location at the prescribed target phase (3).

Received April 19, 2018; accepted after revision July 3, 2018.
Corresponding author: Ji Won Lee, MD, PhD, Department of Radiology, Pusan National University School of Medicine and Medical Research Institute, Pusan National University Hospital, 179 Gudeok-ro, Seo-gu, Busan 49241, Korea.
• Tel: (8251) 240-7354 • Fax: (8251) 244-7534
• E-mail: jw@pusan.ac.kr

Korean Journal of Radiology
KJR

Previous studies have shown MCA's beneficial effect on the image quality of coronary CT angiography in patients with a high heart rate (HR) or without HR control (4, 5). However, most studies were performed with a 64-slice single-source dual-energy CT scanner. Liang et al. (6) demonstrated that the use of MCA on a 256-detector row multi-detector CT scanner could significantly improve image quality and diagnostic performance in patients with HR ≥ 75 beats per minute (bpm). However, the effect of HR on motion correction was not analyzed in their study.

Thus, the purpose of this study was to investigate the efficacy of MCA in improving coronary artery image quality and measurement accuracy using an anthropomorphic dynamic heart phantom and 256-detector row CT scanner.

MATERIALS AND METHODS

Anthropomorphic Dynamic Heart Phantom

An anthropomorphic dynamic heart phantom (PH-48; Kyoto Kagaku Corporation, Kyoto, Japan) was used to simulate different HRs. This phantom consists of a chest phantom, diaphragm, simulated heart, and mechanical system. Four coronary arteries with no stenosis (4 mm in diameter) or variable stenosis degrees (25% stenosis [3 mm], 50% stenosis [2 mm], and 75% stenosis [1 mm]) were attached on the heart phantom (Fig. 1). This dynamic heart phantom was controlled by a tablet personal computer, which enabled selection of variable HRs, ejection fraction, and stroke volume. The ejection fraction was set at 60% and stroke volume, at 70 mL.

CT Scanning Protocols

All CT images were acquired using 256-detector row CT (Revolution CT; GE Healthcare, Waukesha, WI, USA). First, we scanned the cardiac phantom at a static condition to confirm the lumen size and the degree of stenosis in the simulated coronary arteries. Then, we scanned the phantom at eight simulated HRs (50–120 bpm with 10-bpm increments) once each. We used the prospectively electrocardiogram-triggered axial scan during 20–80% of the R-R interval, with a padding of 80 ms for MCA (Snapshot Freeze; GE Healthcare). Other scanning parameters were a tube voltage of 100 kVp, tube current of 228 mA, scan range of 160 mm, and gantry rotation time of 0.28 s/rot. For all HRs, data at 45% of the R-R interval were selected for reconstruction because data at this interval show minimal motion artifacts. The reconstruction interval/slice thickness, weight of the iterative reconstruction (adaptive statistical iterative reconstruction-V), reconstruction matrix, and reconstruction algorithm were 0.625 mm/0.625 mm, 50%, 512 x 512, and standard, respectively. To evaluate the effect of MCA, we reconstructed both images using conventional reconstruction and motion-correction reconstruction for all HRs.

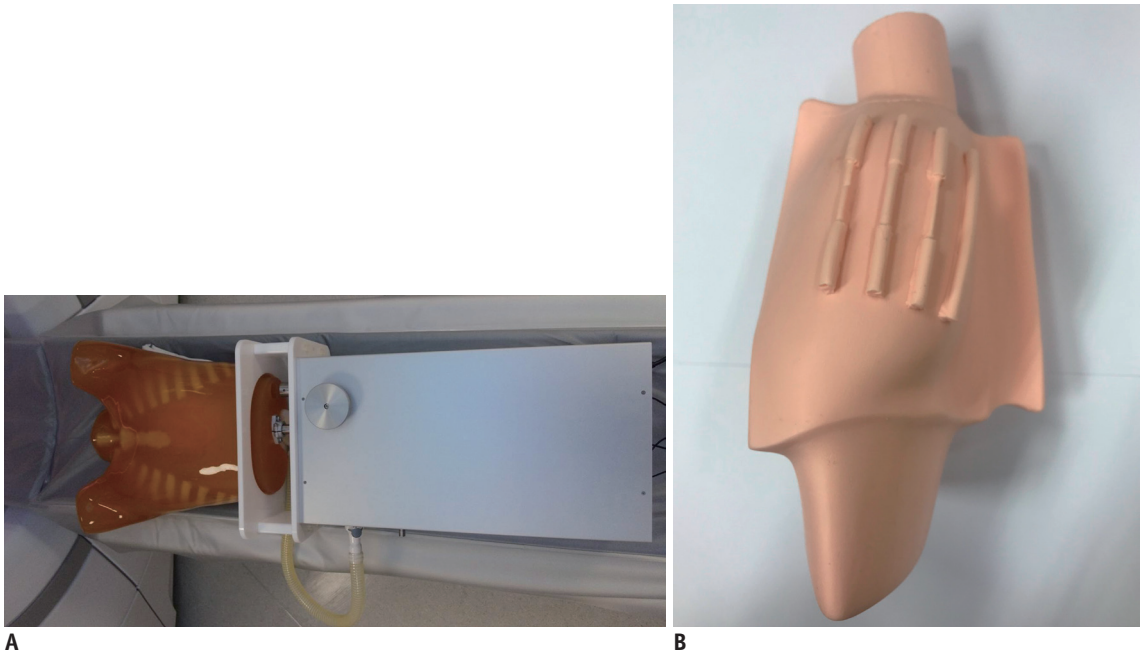

A B

Fig. 1. Anthropomorphic dynamic heart phantom and simulated heart with stenotic model.
A. Anthropomorphic dynamic heart phantom. **B.** Simulated heart with stenotic model.

https://doi.org/10.3348/kjr.2018.0251

Image Analysis of the Coronary Arteries

The reconstructed images were sent to a dedicated work station for image analysis (Advantage Workstation 4.6; GE Healthcare). Images were displayed at a window width of 800 HU and a window level of 100 HU; however, the reviewers were allowed to modify the window width and level for image quality analysis. Image analysis for coronary artery image quality and measurement accuracy was performed by two independent, blinded radiologists who had 10 and 9 years of experience in cardiothoracic imaging, respectively. The average values of the measurements were used for statistical analysis for image quality and measurement accuracy analysis.

Image Quality Analysis

Axial and curved multiplanar reformatted images of the coronary artery were used for subjective analysis of the coronary artery image quality. Image quality was graded using a four-point scale for each level as follows: 1, excellent (no motion artifact); 2, good (minor blurring artifact); 3, fair (moderate blurring artifact); and 4, poor (significant blurring or doubled appearance of structure) (7). Grade 4 was considered to provide non-diagnostic image quality.

Measurement Accuracy

Measurement accuracy was determined using the measurement errors of the minimal luminal diameter (MLD) and minimal luminal area (MLA). Using the dedicated work station, the MLD and MLA in the 12 segments were semi-automatically measured (Fig. 2). The MLD and MLA of each segment were compared with those corresponding to the

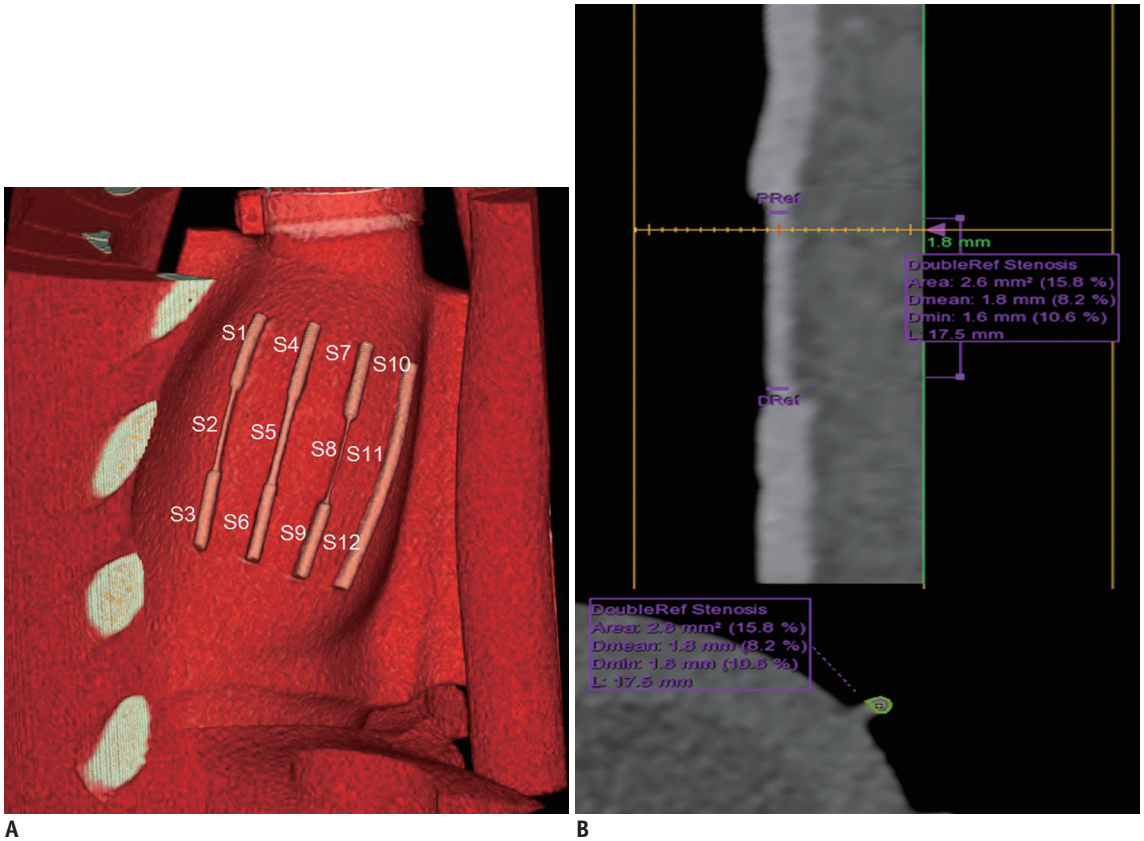

Fig. 2. Volume-rendered curved multiplanar reformatted CT images and transverse section of coronary artery demonstrating segmentations of coronary arteries and measurement of MLD and MLA.

A. Volume-rendering images of heart phantom at HR of 70 bpm demonstrate segmentations of coronary artery. There are 4 coronary arteries in cardiac phantom. Each coronary artery was divided into three segments. Therefore, total of 12 coronary artery segments were analyzed. **B.** Curved multiplanar reformatted CT images and transverse section of S2 illustrating method used to measure MLD and MLA. When PRef and DRef were set for each segment, software automatically measure MDL and MLA of each segment (yellow line represents narrowest level of S2). In case software presented incorrect centerline or outline, observer was able to adjust it. At HR of 70 bpm, MLD and MLA of S2 were 1.6 mm and 2.6 mm^2, respectively. Data in parenthesis (%) represents stenosis percentage using dual reference selection. bpm = beats per minute, CT = computed tomography, Dmean = mean luminal diameter, Dmin = minimal luminal diameter, DRef = distal references, HR = heart rate, L = length, MLA = minimal luminal area, MLD = minimal luminal diameter, PRef = proximal references, S = segment

https://doi.org/10.3348/kjr.2018.0251

Korean Journal of Radiology
KJR

motion-free segment as a reference, and the measurement error was calculated using the following equation (8-10):

$$\text{Measurement error (\%)} = \frac{\text{(Measured degree of each segement - measured degree of motion-free segement) x 100}}{\text{(Measured degree of motion-free segment)}}$$

The measurement errors of the MLD and MLA were compared for all segments at rest and eight stimulated HRs.

Radiation Dose Analysis

The effective radiation dose associated with the CT examination was calculated by multiplying the dose-length product (DLP) by a chest-specific conversion coefficient ($k = 0.014\ mSv \cdot mGy^{-1} \cdot cm^{-1}$), as described by the European Guidelines for Multislice Computed Tomography (11).

Statistical Analysis

Statistical analysis was performed using PASW Statistics software (ver. 18.0; SPSS Inc., Chicago, IL, USA). Continuous variables were expressed as means ± standard deviations and categorical data, as percentages. Inter-observer reproducibility was calculated using the intra-class correlation coefficient (ICC), where ICCs less than 0.50, between 0.50 and 0.75, between 0.75 and 0.90, and greater than 0.90 are indicative of poor, moderate, good, and excellent reliabilities, respectively (12).

The Shapiro-Wilk test was used to assess the normality of continuous variables. To compare the image quality and measurement errors among the eight different HRs, the Kruskal-Wallis test was followed by pair-wise comparisons using the Mann-Whitney test because the raw data were non-normally distributed. The Bonferroni correction, which utilized a stricter *p* value of less than 0.002, was used to evaluate differences in the image quality and measurement errors among the eight HRs. To compare image quality and measurement error between conventional algorithm (CA) and MCA, normally distributed data were tested using a paired Student's *t* test and nonparametric distributed data were tested using a Wilcoxon signed-rank test. A *p* value < 0.05 was considered to indicate statistical significance.

Table 1. Mean Image Quality Scores for CA and MCA (n = 12 Segments for Each HR)

HR (bpm)	CA	MCA	*P*
50	1.1 ± 0.3	1.0 ± 0.1	0.317
60	1.1 ± 0.2	1.1 ± 0.2	1.0
70	1.0 ± 0.1	1.0 ± 0.0	0.317
80	1.0 ± 0.1	1.0 ± 0.0	0.317
90	1.1 ± 0.2	1.0 ± 0.0	0.157
100	1.0 ± 0.1	1.1 ± 0.3	0.317
110	1.9 ± 0.8	1.3 ± 0.3	0.003*
120	2.3 ± 0.6	1.7 ± 0.7	0.006*

Results are means ± standard deviations. *Indicates statistically significant difference ($p < 0.05$). bpm = beat per minute, CA = conventional algorithm, HR = heart rate, MCA = motion-correction algorithm

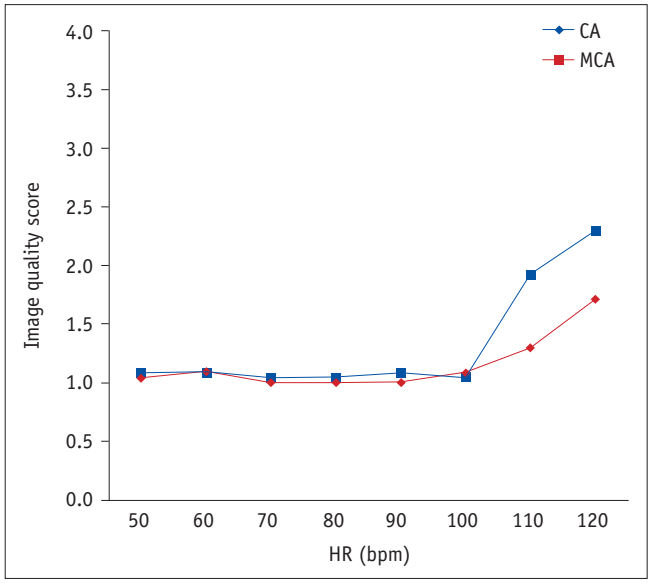

Fig. 3. Mean image quality scores of CA and MCA according to HR. Image quality score at HR of 120 bpm was significantly higher (all *p* values < 0.001) than those at 50–100 bpm according to Kruskal-Wallis test with following pair-wise comparison using Mann-Whitney test and Bonferroni correction. CA = conventional algorithm, MCA = motion correction algorithm

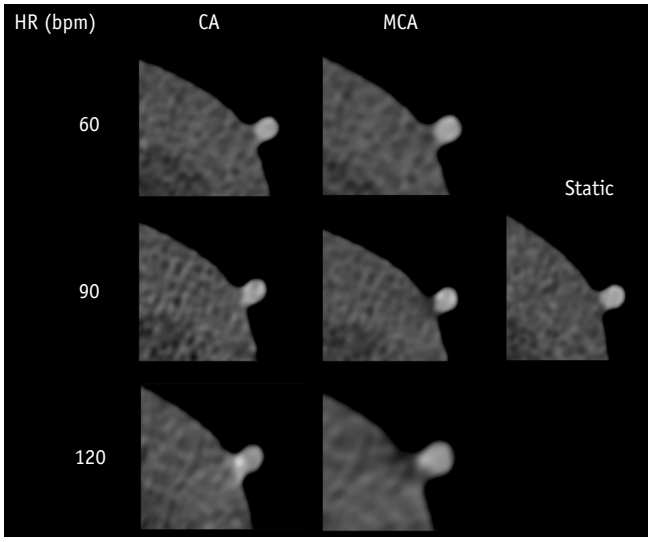

Fig. 4. Representative axial images reconstructed by CA and MCA at HRs of static and 60, 90, and 120 bpm.

https://doi.org/10.3348/kjr.2018.0251

RESULTS

Image Quality Improvement by MCA under Different HRs

There was good inter-observer reproducibility for subjective image quality scoring (ICC = 0.809). Table 1 and Figure 3 show the mean image quality scores of CT images reconstructed by CA and MCA. Image quality scores tended to decrease with higher HRs at 110 bpm and 120 bpm. The Kruskal-Wallis test followed by pair-wise comparison using the Mann-Whitney test and Bonferroni correction showed that the image quality score at 120 bpm was significantly higher than those at 50–110 bpm (all *p* values, < 0.001). At 50–100 bpm, both reconstruction algorithms achieved similar image quality scores. At 110 bpm (1.9 ± 0.8 for CA, 1.3 ± 0.3 for MCA; $p = 0.003$) and 120 bpm (2.3 ± 0.6 for CA, 1.7 ± 0.7 for MCA; $p = 0.006$), MCA achieved better image quality than did CA (Table 1). Using MCA, mean image quality score was improved for all coronary segments at 110 bpm (75% stenosis [3 for CA vs. 1.5 for MCA], 50% stenosis [1.5 for CA vs. 1 for MCA], 25% stenosis [2.5 for CA vs. 1.5 for MCA], no stenosis [1.9 for CA vs. 1.3 for MCA]) and at 120 bpm (50% stenosis [3 for CA vs. 2 for MCA], 25% stenosis [3 for CA vs. 2 for MCA], no stenosis [2.3 for CA vs. 1.7 for MCA]) except for coronary segments with 75% stenosis at 120 bpm (2 for CA vs. 2 for MCA). Figure 4 images reconstructed by CA and MCA at static condition, 60, 90, and 120 bpm also demonstrated reduced motion artifact, with a significant improvement at higher HR. The image interpretability of CA and MCA were 100% at all HRs.

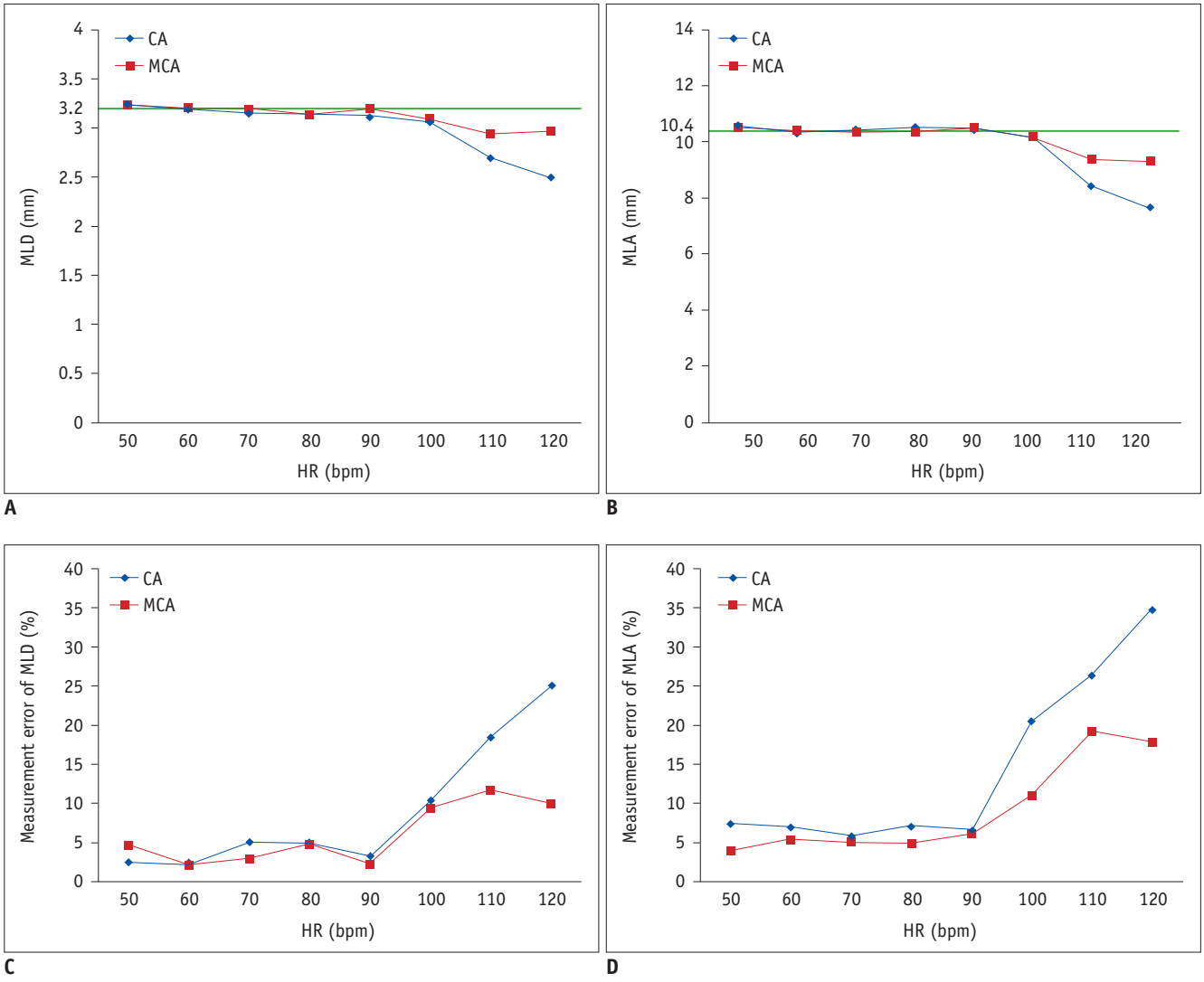

Fig. 5. Measurement accuracy according to HR between CA and MCA.
A. MLD. Green line presents MLD at static (reference, 3.2 mm). **B.** MLA. Green line presents MLA at static (reference, 10.4 mm^2). **C.** Measurement error of MLD. **D.** Measurement error of MLA.

https://doi.org/10.3348/kjr.2018.0251

Korean Journal of Radiology
KJR

Table 2. MLD and Measurement Error of MLD for CA and MCA (n = 12 Segments for Each HR)

HR (bpm)	CA	MCA	*P*
MLD (mm)			
Static	3.2 ± 1.0		
50	3.2 ± 1.0	3.2 ± 1.0	0.87
60	3.2 ± 1.0	3.2 ± 1.0	0.104
70	3.1 ± 1.0	3.2 ± 0.9	0.429
80	3.2 ± 1.0	3.1 ± 1.0	0.755
90	3.1 ± 0.9	3.2 ± 1.0	0.107
100	3.1 ± 0.8	3.1 ± 0.8	0.627
110	2.7 ± 0.7	2.9 ± 0.8	0.012*
120	2.5 ± 1.0	3.0 ± 0.8	0.006*
Measurement error of MLD (%)			
50	2.5 ± 2.6	4.5 ± 4.2	0.165
60	2.2 ± 2.6	2.1 ± 2.5	0.801
70	5.1 ± 7.1	2.9 ± 2.4	0.305
80	4.9 ± 8.4	4.7 ± 5.4	0.678
90	3.3 ± 4.2	2.2 ± 2.5	0.460
100	10.4 ± 7.8	9.4 ± 7.5	0.543
110	18.4 ± 9.4	11.7 ± 5.9	0.013*
120	25.0 ± 16.5	10.0 ± 7.3	0.013*

Results are presented as means ± standard deviations. *Statistically significant difference ($p < 0.05$). MLD = minimal luminal diameter

Table 3. MLA and Relative Error of MLA for CA and MCA (n = 12 Segments for Each HR)

HR (bpm)	CA	MCA	*P*
MLA (mm)			
Static	10.4 ± 4.5		
50	10.6 ± 4.7	10.5 ± 4.6	0.428
60	10.3 ± 4.7	10.4 ± 4.6	0.244
70	10.5 ± 4.6	10.3 ± 4.5	0.156
80	10.6 ± 4.7	10.4 ± 4.5	0.217
90	10.4 ± 4.5	10.5 ± 4.6	0.6
100	10.2 ± 3.8	10.2 ± 4.2	0.967
110	8.4 ± 3.6	9.4 ± 3.9	0.011*
120	7.7 ± 4.2	9.3 ± 4.2	0.016*
Measurement error of MLA (%)			
50	7.4 ± 7.4	4.0 ± 2.8	0.078
60	6.9 ± 6.2	5.4 ± 3.8	0.414
70	5.9 ± 5.0	5.2 ± 5.5	0.563
80	7.0 ± 6.8	4.9 ± 4.2	0.081
90	6.5 ± 4.8	6.3 ± 7.0	0.779
100	20.6 ± 24.7	11.1 ± 11.5	0.152
110	26.4 ± 21.6	19.2 ± 28.1	0.028*
120	34.8 ± 19.6	17.9 ± 17.7	0.018*

Results are presented as means ± standard deviations. *Statistically significant difference ($p < 0.05$). MLA = minimal luminal area

Measurement Accuracy Improvement by MCA under Different HRs

A good to excellent inter-observer reproducibility was observed for MLD (ICC = 0.76) and MLA (ICC = 0.973). Figure 5 shows the MLD, MLA, and their measurement errors. The MLD and MLA of both CA and MCA decreased with higher HRs, while the measurement errors of both CA and MCA increased with higher HRs especially at 110 bpm and 120 bpm. Tables 2 and 3 show that MCA could significantly improve the measurement errors of the MLD and MLA at 110 bpm (measurement error of the MLD, 18.4 ± 9.4% for CA vs. 11.7 ± 5.9% for MCA, $p = 0.013$; measurement error of the MLA 26.4 ± 21.6% for CA vs. 19.2 ± 28.1% for MCA, $p = 0.028$) and 120 bpm (measurement error of the MLD, 25.0 ± 16.5% for CA vs. 10.0 ± 7.3% for MCA, $p = 0.013$; measurement error of MLA, 34.8 ± 19.6% for CA vs. 17.9 ± 17.7% for MCA, $p = 0.018$).

Radiation Dose

The mean DLP was 53.6 ± 3.9 mGy·cm, and the mean effective radiation dose was 0.8 ± 0.1 mSv.

DISCUSSION

This phantom study confirms that 256-detector row CT yields an acceptable image quality of the coronary artery at HR ≤ 120 bpm. MCA significantly increased the image quality score and decreased the measurement error at a high HR.

Motion artifacts are a major factor that limits the image quality of heart CT. To reduce motion artifacts, beta-blocker use is recommended, in accordance with the Society of Cardiovascular Computed Tomography guidelines for performance of and image acquisition by coronary CT angiography (13). However, contraindications to beta-blocker use and lack of treatment response make it impossible to achieve target HRs in some patients. For this reason, several methods have been introduced to improve the diagnostic performance in patients with high HRs. They include the use of dual-source CT, wide-detector CT, increased gantry rotation speed, and image reconstruction during the optimal phase of the cardiac cycle (14-16). A recently developed MCA can further correct the motion artifact by utilizing both coronary artery path and velocity from adjacent cardiac phases in a single cardiac cycle (3).

Prior studies have documented beneficial effects of MCA in terms of image quality and diagnostic accuracy using a pulsating coronary phantom (Mocomo; Fuyo Corp, Tokyo, Japan) (8, 17). Cho et al. (8) demonstrated that the coronary artery image quality and diagnostic accuracy (i.e.,

https://doi.org/10.3348/kjr.2018.0251

measurement errors of the MLA and MLD) improved on using MCA at high HRs (i.e., 80 bpm and 100 bpm), although there was no benefit at low HRs (i.e., 60 bpm). Xing et al. (17) also showed that the coronary artery image quality improved on using MCA at 70–100 bpm (10-bpm interval) on monochromatic levels of 50, 60, and 70 keV in their phantom study using dual-energy spectral CT. Their results have similar trends to our results. However, they used a 64-slice single-source dual-energy CT scanner, and their maximum HR was set at 100 bpm.

Our phantom study used 256-detector row CT with a single heartbeat acquisition. Therefore, the mean effective radiation dose of 0.8 mSv in this study was lower than those of previous studies that evaluated the effect of MCA using 64-slice CT (4, 5, 18, 19). Liang et al. (6) evaluated the effect of MCA on image quality and diagnostic accuracy in patients with high HRs using 256-detector row multi-detector CT. However, the effect of HR on motion correction was not analyzed. Thus, the advantage of our study is that MCA improves the HR-dependent image quality and measurement accuracy using anthropomorphic dynamic heart phantom and 256-detector row CT scanner.

This study has several limitations. First, an anthropomorphic phantom represents a surrogate for actual situations only; thus, the results need to be validated in *in vivo* studies. However, we could avoid the confounders of unexpected arrhythmia, changing HRs due to contrast medium injection, vagal tone during breath-hold, or anxiety because the HRs in our phantom study were well controlled. Second, we evaluated the effect on the image quality and measurement accuracy in a regular heartbeat simulation setting. The effect of MCA in an arrhythmic setting remains to be established. Third, we could not analyze the effect of MCA on subjective image quality and measurement errors of the MLD and MLA according to different stenotic degree using statistical analysis because of small sample size. Finally, we could not evaluate the influence of plaque characteristics on motion correction because our heart phantom has stenotic coronary arteries without a plaque. Further investigation with larger sample size is needed to evaluate the effect of MCA according to stenotic degree and plaque type.

In conclusion, MCA can improve the coronary artery image quality and measurement accuracy at high HRs using an anthropomorphic dynamic heart phantom and 256-detector row CT scanner. Prospective clinical trials should aim at establishing and validating our results in the clinical population setting.

Conflicts of Interest

The authors have no financial conflicts of interest.

ORCID

Ji Won Lee
https://orcid.org/0000-0003-1800-8548
Jeong Bin Park
https://orcid.org/0000-0001-8365-3012

REFERENCES

1. Schroeder S, Kopp AF, Kuettner A, Burgstahler C, Herdeg C, Heuschmid M, et al. Influence of heart rate on vessel visibility in noninvasive coronary angiography using new multislice computed tomography: experience in 94 patients. *Clin Imaging* 2002;26:106-111
2. Hoffmann MH, Shi H, Manzke R, Schmid FT, De Vries L, Grass M, et al. Noninvasive coronary angiography with 16-detector row CT: effect of heart rate. *Radiology* 2005;234:86-97
3. Min JK, Arsanjani R, Kurabayashi S, Andreini D, Pontone G, Choi BW, et al. Rationale and design of the ViCTORY (Validation of an Intracycle CT Motion CORrection Algorithm for Diagnostic AccuracY) trial. *J Cardiovasc Comput Tomogr* 2013;7:200-206
4. Leipsic J, Labounty TM, Hague CJ, Mancini GB, O'Brien JM, Wood DA, et al. Effect of a novel vendor-specific motion-correction algorithm on image quality and diagnostic accuracy in persons undergoing coronary CT angiography without rate-control medications. *J Cardiovasc Comput Tomogr* 2012;6:164-171
5. Andreini D, Pontone G, Mushtaq S, Bertella E, Conte E, Segurini C, et al. Low-dose CT coronary angiography with a novel IntraCycle motion-correction algorithm in patients with high heart rate or heart rate variability. *Eur Heart J Cardiovasc Imaging* 2015;16:1093-1100
6. Liang J, Wang H, Xu L, Dong L, Fan Z, Wang R, et al. Impact of SSF on diagnostic performance of coronary computed tomography angiography within 1 heart beat in patients with high heart rate using a 256-row detector computed tomography. *J Comput Assist Tomogr* 2018;42:54-61
7. Farshad-Amacker NA, Alkadhi H, Leschka S, Frauenfelder T. Effect of high-pitch dual-source CT to compensate motion artifacts: a phantom study. *Acad Radiol* 2013;20:1234-1239
8. Cho I, Elmore K, Ó Hartaigh B, Schulman-Marcus J, Granser H, Valenti V, et al. Heart-rate dependent improvement in image quality and diagnostic accuracy of coronary computed tomographic angiography by novel intracycle motion correction algorithm. *Clin Imaging* 2015;39:421-426
9. Toepker M, Euller G, Unger E, Weber M, Kienzl D, Herold CJ, et al. Stenosis quantification of coronary arteries in coronary

https://doi.org/10.3348/kjr.2018.0251

vessel phantoms with second-generation dual-source CT: influence of measurement parameters and limitations. *AJR Am J Roentgenol* 2013;201:W227-W234
10. Wang YT, Yang CY, Hsiao JK, Liu HM, Lee WJ, Shen Y. The influence of reconstruction algorithm and heart rate on coronary artery image quality and stenosis detection at 64-detector cardiac CT. *Korean J Radiol* 2009;10:227-234
11. ICRP. The 2007 recommendations of the International Commission on Radiological Protection. ICRP Publication 103. *Ann ICRP* 2007;37:1-332
12. Koo TK, Li MY. A guideline of selecting and reporting intraclass correlation coefficients for reliability research. *J Chiropr Med* 2016;15:155-163
13. Abbara S, Blanke P, Maroules CD, Cheezum M, Choi AD, Han BK, et al. SCCT guidelines for the performance and acquisition of coronary computed tomographic angiography: a report of the Society of Cardiovascular Computed Tomography Guidelines Committee: endorsed by the North American Society for Cardiovascular Imaging (NASCI). *J Cardiovasc Comput Tomogr* 2016;10:435-449
14. Achenbach S, Marwan M, Schepis T, Pflederer T, Bruder H, Allmendinger T, et al. High-pitch spiral acquisition: a new scan mode for coronary CT angiography. *J Cardiovasc Comput Tomogr* 2009;3:117-121
15. Rybicki FJ, Otero HJ, Steigner ML, Vorobiof G, Nallamshetty L, Mitsouras D, et al. Initial evaluation of coronary images from 320-detector row computed tomography. *Int J Cardiovasc Imaging* 2008;24:535-546
16. Achenbach S, Ropers U, Kuettner A, Anders K, Pflederer T, Komatsu S, et al. Randomized comparison of 64-slice single- and dual-source computed tomography coronary angiography for the detection of coronary artery disease. *JACC Cardiovasc Imaging* 2008;1:177-186
17. Xing Y, Zhao Y, Guo N, Pan CX, Azati G, Wang YW, et al. Effect of a novel intracycle motion correction algorithm on dual-energy spectral coronary CT angiography: a study with pulsating coronary artery phantom at high heart rates. *Korean J Radiol* 2017;18:881-887
18. Li ZN, Yin WH, Lu B, Yan HB, Mu CW, Gao Y, et al. Improvement of image quality and diagnostic performance by an innovative motion-correction algorithm for prospectively ECG triggered coronary CT angiography. *PLoS One* 2015;10:e0142796
19. Lee H, Kim JA, Lee JS, Suh J, Paik SH, Park JS. Impact of a vendor-specific motion-correction algorithm on image quality, interpretability, and diagnostic performance of daily routine coronary CT angiography: influence of heart rate on the effect of motion-correction. *Int J Cardiovasc Imaging* 2014;30:1603-1612

 https://doi.org/10.3348/kjr.2018.0251